



Synthesis, physicochemical studies, embryos toxicity and DNA interaction of some new Iron(II) Schiff base amino acid complexes

Laila H. Abdel-Rahman*, Rafat M. El-Khatib, Lobna A.E. Nassr, Ahmed M. Abu-Dief

Chemistry Department, Faculty of Science, Sohag University, Sohag 82534, Egypt

H I G H L I G H T S

- ▶ Some novel Fe(II) Schiff base amino acid complexes were prepared and characterized.
- ▶ The stoichiometry and stability of the complexes were determined spectrophotometrically.
- ▶ The embryos toxicity of the studied complexes was tested on chick embryos.
- ▶ The interaction between CT-DNA and the complexes was studied.

A R T I C L E I N F O

Article history:

Received 10 January 2013

Received in revised form 19 February 2013

Accepted 19 February 2013

Available online 26 February 2013

Keywords:

Schiff base

Amino acid

Fe(II) complexes

Toxicity

DNA interaction

A B S T R A C T

New Fe(II) Schiff base amino acid complexes derived from the condensation of *o*-hydroxynaphthaldehyde with *L*-alanine, *L*-phenylalanine, *L*-aspartic acid, *L*-histidine and *L*-arginine were synthesized and characterized by elemental analysis, IR, electronic spectra, and conductance measurements. The stoichiometry and the stability constants of the complexes were determined spectrophotometrically. The investigated Schiff bases exhibited tridentate coordination mode with the general formulae $[\text{Fe}(\text{HL})_2] \cdot n\text{H}_2\text{O}$ for all amino acids except *L*-histidine. But in case of *L*-histidine, the ligand acts as tetradentate ($[\text{FeL}(\text{H}_2\text{O})_2] \cdot 2\text{H}_2\text{O}$), where HL = mono anion and L = dianion of the ligand. The structure of the prepared complexes is suggested to be octahedral. The prepared complexes were tested for their toxicity on chick embryos and found to be safe until a concentration of 100 $\mu\text{g}/\text{egg}$ with full embryos formation. The interaction between CT-DNA and the investigated complexes were followed by spectrophotometry and viscosity measurements. It was found that, the prepared complexes bind to DNA via classical intercalative mode and showed a different DNA cleavage activity with the sequence: $\text{nhi} > \text{nari} > \text{nali} > \text{nasi} > \text{nphali}$. The thermodynamic Profile of the binding of *nphali* complex and CT-DNA was constructed by analyzing the experimental data of absorption titration and UV melting studies with the McGhee equation, van't Hoff's equation, and the Gibbs–Helmholtz equation.

© 2013 Elsevier B.V. All rights reserved.

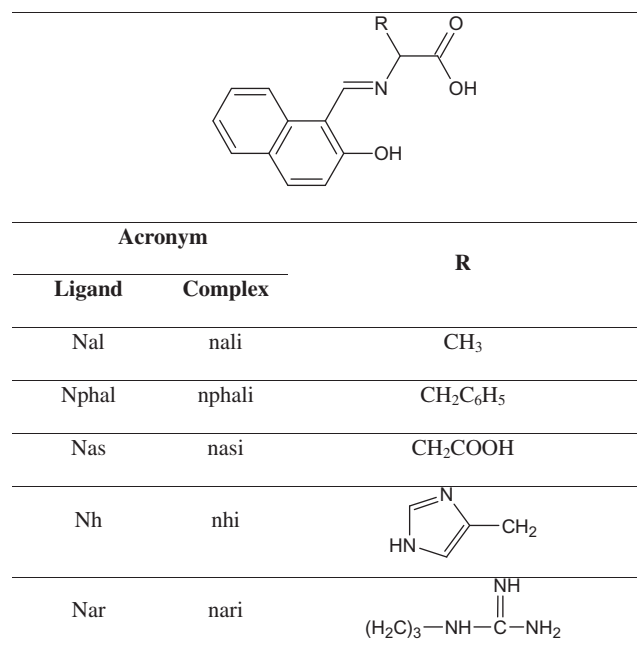
1. Introduction

Schiff base metal complexes have been studied extensively because of their remarkable chemical and physical properties. Metal complexes of Schiff base phenolates with favorable cell membrane permeability have been exploited in cancer multidrug resistance [1] and used as antimalarial agents [2]. Schiff base amino acid complexes have gained importance from the inorganic point of view and owing to their physiological and pharmacological activities [3,4]. Moreover, metal chelates of Schiff bases derived from *o*-hydroxy aromatic aldehydes, e.g. *o*-hydroxynaphthaldehyde and amino acids have some relationship to ligands involved in a variety of biological processes, e.g. transamination, racemization and car-

boxylation [5]. Furthermore, Schiff base complexes have an extensive importance in many fields such as radiotracers [6], biologically active reagents [7–10], catalysts in many number of homogeneous and heterogeneous reactions such as oxidation [11–13], epoxidation [14,15], polymerization [16,17] and decomposition reactions [18–20]. Little effort has been expended to prepare Fe(II) amino acid Schiff base complexes [21–23] regardless of their importance as complexes containing a metal in a very sparingly stable low oxidation state, in addition to connecting unstable ligands. Studying the interaction between transition metal complexes and DNA has attracted many interests [24–31] due to their importance in cancer therapy, design of new types of pharmaceutical molecules and molecular biology. On the other hand, few studies were carried out concerning the interaction of DNA with Schiff base amino acid complexes [32].

* Corresponding author. Fax: +20 93 4 601 159.

E-mail address: lailakenwy@hotmail.com (L.H. Abdel-Rahman).



Scheme 1. Structures and abbreviations of the Schiff base ligands and their corresponding complexes.

Therefore, in the present work some novel Fe(II) Schiff base amino acid complexes were prepared and characterized by various physical methods to obtain more information and indicate their structures and behavior. Moreover, the teratogenicity of the studied complexes was tested on chick embryos to check the safety of these compounds in the human body. Furthermore, the interaction between native calf thymus deoxyribonucleic acid (CT-DNA) and the investigated complexes was performed by spectrophotometric and viscosity measurements. The aldehyde used in this investigation is 2-hydroxy-1-naphthaldehyde and the amino acids are L-alanine (ala), L-phenylalanine (phala), L-aspartic acid (aspa), L-histidine (his) and L-arginine (arg). The structures of the Schiff base amino acid ligands studied in this investigation are shown in Scheme 1.

2. Experimental

All chemicals used in this investigation such as 2-hydroxy-1-naphthaldehyde, amino acids, the metal salt ($\text{FeSO}_4 \cdot (\text{NH}_4)_2 \text{SO}_4 \cdot 6\text{H}_2\text{O}$) Calf thymus DNA (CT-DNA) and Tris[hydroxymethyl]aminomethane (Tris) were obtained from Sigma–Aldrich. Spectroscopic grade ethanol product was used.

2.1. Synthesis of Schiff base amino acid ligands

Schiff bases under investigation were prepared according to the procedure previously described in the literature [33]. By adding 3 mmol of the 2-hydroxy-1-naphthaldehyde was dissolved in 40 ml ethanol and then added to 3 mmol of the amino acid (ala, phala, aspa, his or arg) solution in aqueous-ethanol mixture. The mixture was refluxed for 5 h, the solvent was removed on a rotary evaporator and the residue crystallized at room temperature. After leaving the solution for one day at room temperature, yellow crystals in case of L-alanine, L-phenylalanine and L-aspartic acid were formed. Whereas, brown and green crystals were obtained in the case of L-histidine and L-arginine, respectively. The precipitate was recrystallized from ethanol / diethyl ether.

2.2. Synthesis of the complexes

Ethanollic ligand solution was treated with ethanollic solution of 5 mmol $\text{FeSO}_4 \cdot (\text{NH}_4)_2 \text{SO}_4 \cdot 6\text{H}_2\text{O}$. To avoid oxidation of Fe(II), a few drops of glacial acetic acid were added [21]. The resulting solution was stirred magnetically for 12 h at 25 °C and then evaporated over night. Afterthat, the resulted solid product was filtered, washed with water and dry ether, respectively and finally dried in desiccator.

2.3. Physical measurements

Conductivity measurements were carried out using JENWAY conductivity meter model 4320 at 298 K using ethanol as solvent. The electronic spectra of the complexes using ethanol as solvent were monitored using 10 mm matched quartz cells on Jasco UV–Visible spectrophotometer model V-530. IR spectra of the metal chelates were monitored using Shimadzu FTIR model 8101 in the region 4000–400 cm^{-1} using dry KBr discs. Elemental analyses were carried by Elemental analyzer perkin-Elmer model 240c. Magnetic moment measurements of the investigated complexes were carried out on a vibrating sample magnetometer (VSM). The values of absorbance of 5×10^{-3} M of each complex were measured at different values of pH obtained by preparing a series of Britton universal buffer [34] was used. pH measurements were carried out using HNNNA 211 pH meter at 298 K.

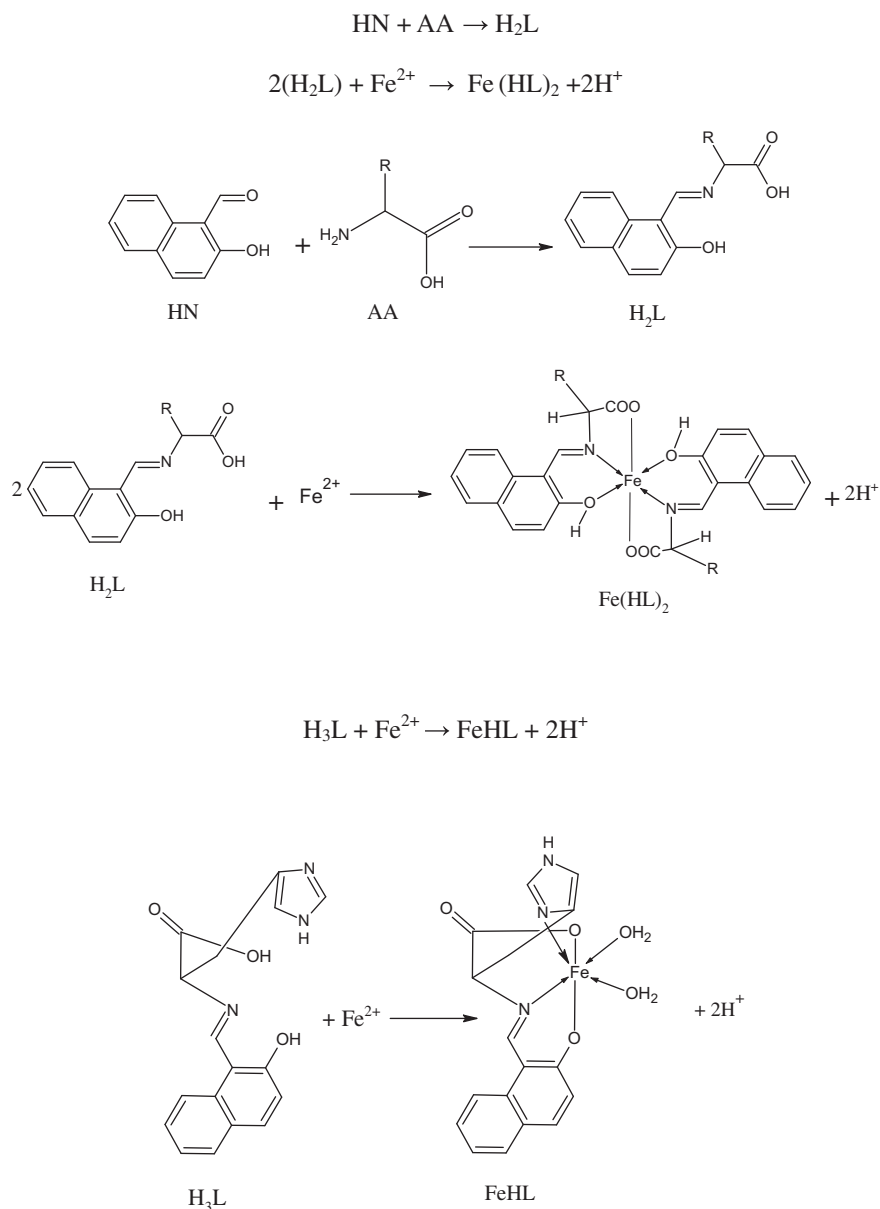
2.4. Embryos toxicity

The toxicity of the prepared complexes at different concentrations (5, 10, 20, 40, 100 and 200 $\mu\text{g}/\text{egg}$) were investigated by exploration of their administration to developing chicken embryos for 17 days at 37 °C in incubation. All eggs were turned with a quick movement of the wrist and left to lie horizontally 24 h before injection to let the germ cells float free to the top of the yolk and avoid trauma during the injection procedure. The day of injection was denoted as day 0. The eggshell was wiped with a tissue with 70% ethanol, and a 2 mm. hole was drilled over the air chamber, not penetrating the membrane. Then, the eggshell was wiped with 70% ethanol again, and 50 μl of the complex solution was injected into the yolk. Exposure doses were 5, 10, 20, 40, 100 and 200 $\mu\text{g}/\text{egg}$ of each complex. Once removed from the incubator, eggs were opened and embryos were sacrificed by decapitation. The embryos were weighed and compared to a reference sample injected only with the solvent. Differences in the uptake of the investigated complexes might not be attributed to differences in egg weight because eggs were weighed and randomly assigned to treatment groups; initial egg weights did not differ among groups. Statistical analysis was carried out to evaluate the significant and insignificant changes compared with the control using student T test.

2.5. Interaction with Calf Thymus DNA (CTDNA)

2.5.1. DNA binding analysis using electronic spectra

The interaction of the prepared complexes with DNA were carried out in Tris-HCl buffer (50 mM, pH 7.2). Calf thymus DNA (CT-DNA) was purified by centrifugal dialysis before use. CT-DNA solution at pH = 7.5 gives a ratio of UV absorbance at 260 and 280 nm of about >1.86, indicating that the DNA was sufficiently free from protein contamination [35,36]. The concentration of CT-DNA was determined by monitoring the UV absorbance at 260 nm using $\epsilon_{260} = 6600 \text{ mol}^{-1} \text{ cm}^2$. The stock solution was stored at 4 °C and used within one only day. The spectrophotometric titration was done by maintaining the concentration of the complex constant and varying the concentration of CT-DNA in interaction medium. The absorption of free CT-DNA was canceled by adding an



Scheme 2. Formation of the investigated Schiff base amino acid ligands and their complexes (HN = 2-hydroxy-1-naphthaldehyde, AA = amino acid, H₂L = nal, nphal, nas and nar ligands, H₃L = nh ligand, Fe(HL)₂ = nali, nphali, nasi, nari complexes and FeHL = nhi complex).

Table 1
Analytical and physical data for the Schiff base amino acid ligands and their Fe(II) complexes.

Compound	Empirical formula (formula weight)	Yield (%)	Molar conductance Λ_m ($\Omega^{-1} \text{ cm}^2 \text{ mol}^{-1}$)	Decom. temp. ($^{\circ}\text{C}$)	Analysis found (Calculated)		
					C	H	N
nal	C ₁₄ H ₁₃ NO ₃ (243.254)	83		162	69.25 (69.12)	5.17 (5.39)	5.61 (5.76)
nali	C ₂₈ H ₂₈ FeN ₂ O ₈ (576.37)	75	35.12	260	58.50 (58.34)	4.67 (4.90)	4.88 (4.86)
nphal	C ₂₀ H ₁₇ NO ₃ (319.346)	85		170	75.35 (75.22)	5.21 (5.37)	4.45 (4.39)
nphali	C ₄₀ H ₃₄ FeN ₂ O ₇ (710.54)	83	28.24	>350	67.85 (67.61)	4.57 (4.82)	3.76 (3.94)
nas	C ₁₅ H ₁₃ NO ₅ (287.168)	73		97	62.81 (62.73)	4.63 (4.56)	4.72 (4.88)
nasi	C ₃₀ H ₂₆ FeN ₂ O ₁₁ (646.38)	72	39.31	185	56.01 (55.74)	3.92 (4.05)	4.21 (4.33)
nh	C ₁₇ H ₁₅ N ₃ O ₃ (309.32)	85		156	66.13 (66.01)	4.72 (4.89)	13.44 (13.59)
nhi	C ₁₇ H ₂₁ FeN ₃ O ₇ (435.22)	81	47.61	>350	46.83 (46.91)	4.72 (4.86)	9.58 (9.66)
nar	C ₁₇ H ₂₀ N ₄ O ₃ (328.37)	86		133	62.29 (62.18)	6.05 (6.14)	17.21 (17.07)
nari	C ₃₄ H ₄₄ FeN ₈ O ₉ (764.62)	84	32.21	235	53.64 (53.40)	5.72 (5.80)	14.43 (14.66)

equimolar CT-DNA to pure buffer solution in the reference compartment and the resulting spectra were believed to be result from the metal complexes and the DNA-metal complex aggregates.

From the absorption data, the intrinsic binding constant (K_b) was determined by plotting $[\text{DNA}]/(\varepsilon_a - \varepsilon_f)$ versus $[\text{DNA}]$ according to the following equation:

Table 2
The infrared absorption frequencies (cm^{-1})^a of the investigated Schiff base amino acid ligands and their Fe(II) complexes.

Schiff base ligands and their complexes	Assignment											
	$\nu(\text{OH}); \text{H}_2\text{O}$	$\nu(\text{—C=N})$ stretching	$\nu(\text{C=C})$ stretching	$\nu(\text{C—H})$ aromatic	$\nu(\text{C—H})$ aliphatic	$\nu(\text{COO—})$ symmetric stretching	$\nu(\text{COO}^-)$ asymm.	$\nu(\text{C—O})$ phenolic	$\nu(\text{Fe—N})$	$\nu(\text{Fe—O})$	$\nu(\text{—NH}_2)$ stretching	$\nu(\text{—NH})$ stretching
nal	3403 (w)	1630 (s)	1458 (s)	3081 (w)	2812 (w)	1413 (m)	1528 (w)	1362 (m)	—	—	—	—
nali	3439 (m)	1622 (s)	1450 (s)	3061 (w)	2924 (w)	1395 (m)	1548 (w)	1314 (m)	522 (w)	490 (m)	—	—
nphal	3466 (w)	1624 (s)	1500 (m)	3121 (w)	2879 (w)	1405 (w)	1597 (m)	1326 (m)	—	—	—	—
nphali	3440 (m)	1614 (s)	1448 (m)	3057 (w)	2923 (w)	1394 (w)	1542 (w)	1315 (w)	559 (w)	497(m)	—	—
nas	3440 (m)	1640 (s)	1462 (m)	3062 (w)	2883 (w)	1462 (m)	1590 (w)	1319 (m)	—	—	—	—
nasi	3430 (m)	1629 (s)	1463 (s)	3064 (w)	2900 (w)	1404 (w)	1550 (w)	1311 (m)	550 (w)	482 (m)	—	—
nh	3421 (m)	1626 (s)	1469 (w)	3025 (w)	2922 (w)	1370 (m)	1531 (w)	1352 (m)	—	—	—	3138 (m)
nhi	3405 (w)	1610 (s)	1459 (m)	3015 (w)	2920 (w)	1360 (m)	1537 (w)	1294 (w)	563 (m)	491 (m)	—	3165 (m)
nar	3413 (w)	1639 (s)	1479 (w)	3058 (w)	2935 (w)	1377 (m)	1577 (w)	1341 (w)	—	—	3332 (m)	3145 (m)
nari	3421 (w)	1630 (s)	1451 (s)	3039 (sh)	2937 (w)	1361 (w)	1537 (w)	1296 (m)	553 (w)	465 (w)	3350 (m)	3172 (m)

^a s = Strong, m = medium, w = weak.

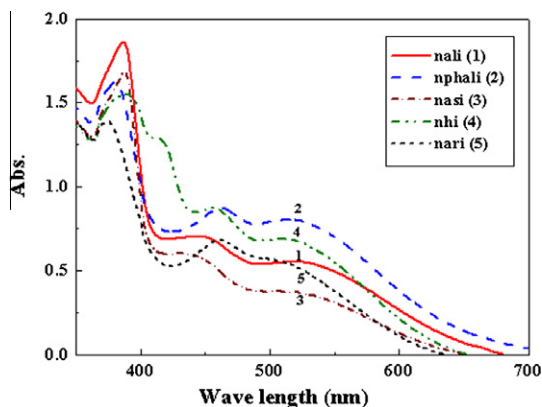


Fig. 1. Molecular electronic spectra of (1) [nali] = 5×10^{-4} mol dm⁻³, (2) [nphali] = 2.5×10^{-4} mol dm⁻³, (3) [nasi] = 5.4×10^{-4} mol dm⁻³, (4) [nhi] = 5×10^{-4} mol dm⁻³ and (5) [nari] = 6×10^{-4} mol dm⁻³.

$$\frac{[\text{DNA}]}{(\varepsilon_a - \varepsilon_f)} = \frac{[\text{DNA}]}{(\varepsilon_b - \varepsilon_f)} + \frac{1}{[K_b(\varepsilon_b - \varepsilon_f)]}$$

where [DNA] is the concentration of DNA in base pairs, the apparent absorption coefficients ε_a , ε_f and ε_b are correspond to $A_{\text{obs}}/[\text{complex}]$, the extinction coefficient for the free complex and extinction coefficient for the complex in fully bound form, respectively. The data were fitted to the above equation with a slope equal to $1/(\varepsilon_b - \varepsilon_f)$ and y-intercept equal to $1/[K_b(\varepsilon_b - \varepsilon_f)]$ and K_b was obtained from the ratio of the slope to the intercept [37]. The standard Gibbs free energy for DNA binding was calculated from the following relation [31]: $\Delta G_b = -RT \ln K_b$.

2.5.2. DNA melting studies

The stability of a DNA double helix can be evaluated by UV melting study technique UV melting studies were carried out using a Jasco UV-Visible spectrophotometer model V-530 spectrophotometer equipped with a Peltier temperature programmer PTP-6. CT-DNA were used in this study. Solutions of DNA in the absence and presence of Fe(II) complex with a [complex]/[DNA-base pair] of 1:1 were prepared in 5 mM Tris, 50 mM NaCl, pH 7.2. The temperature of the solution was increased at 1°C min^{-1} , and the absorbance at 265 nm was continuously monitored.

Table 3
Molecular electronic spectra of the prepared Schiff base amino acid ligands and their Fe(II) complexes.

Compound	λ_{max} , nm ^a	ε_{max} , mol ⁻¹ cm ²	Assignment
nal	256	1614	$\pi-\pi^*$
	292	1600	$\pi-\pi^*$
	392	1690	$n-\pi^*$
	412	932	$n-\pi^*$
	412	932	$n-\pi^*$
nali	390	3740	Intraligand band
	455	1404	LMCT band
	520 (b)	1108	d-d band
	258	1653	$\pi-\pi^*$
	292	1640	$\pi-\pi^*$
nphal	396	1800	$n-\pi^*$
	430	1970	$n-\pi^*$
	380	6520	Intraligand band
	462	3488	LMCT band
	516 (b)	3212	d-d band
nasi	256	1650	$\pi-\pi^*$
	292	1630	$\pi-\pi^*$
	349	1770	$n-\pi^*$
	414	1070	$n-\pi^*$
	380	3148	Intraligand band
nhi	430	1113	LMCT band
	502 (b)	704	d-d band
	256	1641	$\pi-\pi^*$
	292	1640	$\pi-\pi^*$
	396	1800	$n-\pi^*$
nari	424	1960	$n-\pi^*$
	456	522	$n-\pi^*$
	480	435	$n-\pi^*$
	388	3200	Intraligand band
	414 (sh), 456	2500,1746	LMCT band
nar	508 (b)	1380	d-d band
	258	1620	$\pi-\pi^*$
	306	1540	$n-\pi^*$
	398	1728	$n-\pi^*$
	420	1850	$n-\pi^*$
nari	376	2667	Intraligand band
	462	1472	LMCT band
	494 (b)	1288	d-d band

^a b = Broad, sh = shoulder.

2.5.3. DNA binding analysis using viscosity measurements

Viscosity measurements were carried out using an Oswald type viscometer, thermostated at $25 \pm 1^\circ\text{C}$. The flow times were recorded with a digital stopwatch operated timer for different concentrations of the complex (10–250 μM), maintaining the

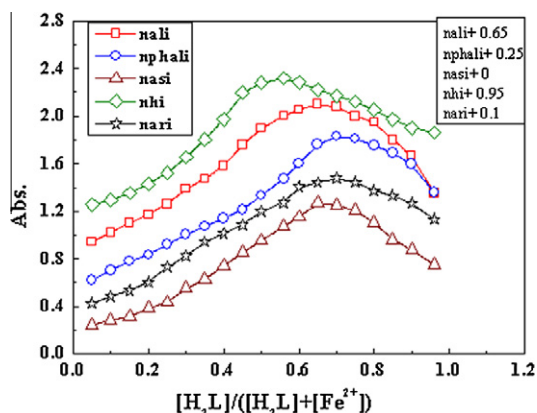


Fig. 2. Continuous variation plots for the prepared complexes in aqueous-alcoholic mixture at $[nali] = 3 \times 10^{-3}$ M, $[npnali] = 3 \times 10^{-3}$ M, $[nasi] = 5 \times 10^{-3}$ M, $[nhi] = 2 \times 10^{-3}$ M, $[nari] = 1 \times 10^{-3}$ M and 298 K.

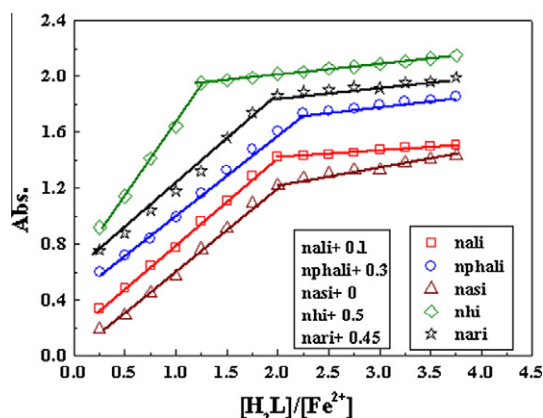


Fig. 3. Molar ratio plots for the studied complexes in aqueous-alcoholic mixture at $nali, npnali: [Fe^{2+}] = 6 \times 10^{-4}$ M; $nasi: [Fe^{2+}] = 1 \times 10^{-3}$ M; $nhi: [Fe^{2+}] = 4 \times 10^{-4}$ M; $nari: [Fe^{2+}] = 1 \times 10^{-3}$ M and 298 K.

concentration of DNA constant (250 μ M). The average value of the three measurements was used to determine the viscosity of the samples. The buffer flow time was recorded as t° . The relative viscosity values for DNA in the presence (η) and absence (η°) of the complex were calculated using the relation $\eta = (t - t^\circ)/t^\circ$, where t is the observed flow time in seconds. The values of relative viscosity (η/η°) were plotted against $1/R$ ($R = [DNA]/[Complex]$) [38].

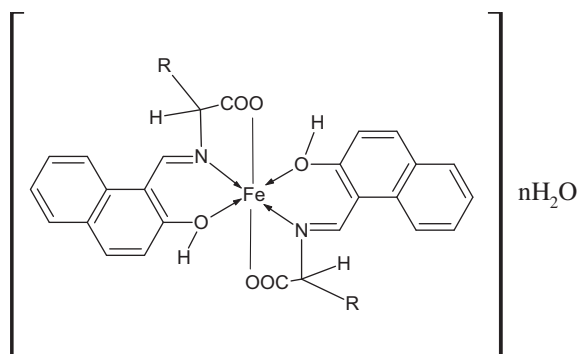
3. Results and discussion

The formation of the investigated Schiff base amino acid ligands and their complexes is represented in Scheme 2 [21].

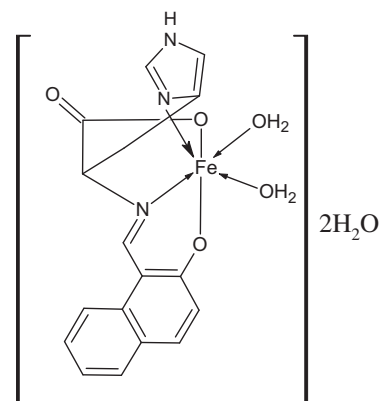
3.1. Identification of the prepared complexes

3.1.1. Microanalyses and molar conductance measurements

The microanalyses results of the prepared Schiff base ligands and their complexes are recorded in Table 1 and suggested that Schiff base ligands act as tridentate and form complexes in 1:2 ratio metal to ligand in case of (ala, phala, asp, arg) while act as tetradentate and form complexes in 1:1 ratio metal to ligand in case of (his). Thus the general formula of the prepared complexes is suggested to be $[Fe(HL)_2] \cdot nH_2O$ and $[FeL(H_2O)_2] \cdot 2H_2O$. To prove the presence of water as coordinated or crystalline water, the prepared complexes are heated at 110 and 160 $^\circ$ C for about 2 h and the



Scheme 3. The suggested structures of nali, npnali, nasi and nari complexes, nali: $n = 2$, npnali and nasi: $n = 1$, nari: $n = 3$, (R as shown in Scheme 1).



Scheme 4. The suggested structure of nhi complex.

obtained weight loss percent data at 110 and 160 $^\circ$ C (for crystallization and coordination water, respectively) were consistent with the corresponding microanalytical data. The following is a comparison among the thermogravimetric data at 110 $^\circ$ C and microanalytical data for crystallization water in the prepared complexes: [nali: 6.20 (6.25)%; npnali: 2.53 (2.35)%; nasi: 2.79 (2.79)%; nhi: 8.25 (8.28)%; nari: 6.95 (7.07)]. Moreover, a comparison among the thermogravimetric data at 160 $^\circ$ C and microanalytical data is reported for coordination water, in the case of the complex nhi: 16.65 (16.66)% that is corresponding to four H_2O molecules, two of them are coordinated and the others are hydrated.

The measured molar conductance values of 10^{-3} molar solutions of the prepared Fe(II) complexes in ethanol were found to be in the range 28.24–47.61 $\Omega^{-1} \text{ cm}^2 \text{ mol}^{-1}$ (cf. Table 1) indicating that the complexes are non-electrolytic in nature.

3.1.2. Infrared spectra

The characteristic vibrations of the free ligand were shifted upon complex formation. A shift to lower frequency, relative to the free Schiff base ligands, of about 8–16 cm^{-1} for the $-C=N$ stretching vibration in the complexes showed that coordination occurs through the nitrogen atoms of the azomethine groups [39]. In the IR spectra of the Schiff bases, the strong absorptions at 1528–1597 and 1370–1405 cm^{-1} are attributed to the asymmetric and symmetric $\nu(\text{COO})$ bands, respectively. These bands shifted to lower frequency values upon complexation indicating that the azomethine nitrogen and the oxygen atom of the carboxylate group are coordinated to the metal ion [40,41] (cf. Table 2).

The recorded IR spectra of the prepared complexes (cf. Table 2) exhibited broad band at 3440–3405 cm^{-1} that assigned to $\nu(\text{OH})$

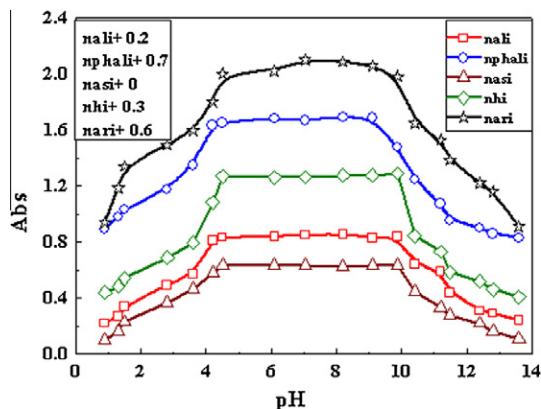


Fig. 4. Dissociation curve of the prepared complexes in aqueous alcoholic mixture at [complex] = 5×10^{-3} M and 298 K.

Table 4

The formation constant (K_f), stability constant (pK) and Gibbs free energy (ΔG°) values of the prepared complexes in aqueous-ethanol at 298 K.

Complex	Type of complex	K_f	pK	ΔG° kJ mol $^{-1}$
nali	1:2	1.29×10^{10}	10.11	-57.68
nphali	1:2	7.81×10^9	9.89	-55.44
nasi	1:2	1.14×10^9	9.06	-51.67
nhi	1:1	6.13×10^5	5.79	-33.02
nari	1:2	4.47×10^{10}	10.65	-60.76

vibration of water molecules associated with the complexes which are confirmed by the elemental and thermal analyses listed in Table 1 [21,42]. A strong band at 1630–1610 cm^{-1} of the complexes can be evidently attributed to $\nu(\text{C}=\text{N})$ vibration, which indicates the presence of an imine structure [43,44]. In nasi complex, $\nu(\text{C}=\text{O})$ vibration band of the coordinated $\beta\text{-COOH}$ group of aspartic acid band is obscured because of the strong $\nu(\text{C}=\text{N})$ vibration band. The shift of this band to lower frequency than that expected (1700 cm^{-1}) may be presumably ascribed to the interaction with the water of hydration through hydrogen bonding. A band appearing at 1550–1537 cm^{-1} may be assigned to $\nu(\text{COO}^-)_{\text{asym}}$ vibrations, while $(\text{COO}^-)_{\text{sym}}$ vibrations appearing at 1404–1361 cm^{-1} . $\Delta\nu(\text{COO}^-) \sim 200 \text{ cm}^{-1}$ indicates the unidentified of the carboxylate group [42,45]. It is worth noting that the asymmetric vibration band of COO^- is obscured by the high intensity of the band of $\text{C}=\text{C}$ stretching vibration at 1462–1448 cm^{-1} [46]. All complexes showed an absorption band in the region of 1315–1294 cm^{-1} that may be attributed to $\nu(\text{CO})$ (phenolic) vibration [42,47]. The bands observed in the region 2937–2900 cm^{-1} and the region 3064–3015 cm^{-1} may be assigned to $\nu(\text{C}-\text{H})$ aliphatic and $\nu(\text{C}-\text{H})$ aromatic stretching vibrations, respectively [48]. The IR bands at 3172 and 3350 cm^{-1} for the nari complex containing arginine moiety are assignable to the terminal guanidinium group [44]. Far-IR of the compounds showed bands in 563–550 and 497–465 cm^{-1}

Table 5

P-values^a for Teratogenicity testing of the investigated complexes compared to control and the used solvent.

Concentration $\mu\text{g}/\text{egg}$	Complex				
	nali	nphali	nasi	nhi	nari
5	0.17	0.59×10^{-1}	0.14	0.85×10^{-1}	
10	0.85	1.24×10^{-2}	3.85×10^{-1}	22.24×10^{-2}	
20	0.67×10^{-1}	0.33×10^{-2}	0.21×10^{-1}	0.11×10^{-2}	
40	0.11×10^{-1}	0.99×10^{-3}	0.27×10^{-2}	35.92×10^{-3}	
100	0.01×10^{-1}	0.12×10^{-3}	0.43×10^{-3}	3.11×10^{-3}	
200	0.11×10^{-2}	40% Embryo resorbed	0.48×10^{-4}	1.92×10^{-4}	

^a $P > 0.05$ (insignificant), $P < 0.05$ (significantly different).

regions that may be attributed to $\nu(\text{Fe}-\text{N})$ and $\nu(\text{Fe}-\text{O})$ stretching, respectively [49,50].

Histidine is believed to have significantly different properties compared with the other amino acids because of the presence of an imidazole ring containing two nitrogen atoms, one of nitrogen atom which protonates in the biologically significant pH ranges of 6–7. This nitrogen atom may strongly coordinate to transition metal ions [51]. This trend confirmed the participation of protonated nitrogen in coordination in nhi complex.

3.1.3. Electronic spectra

To propose a geometrical structure of the designed Fe(II) Schiff base amino acid complexes, the electronic absorption spectra of ethanolic solutions of the ligands and their complexes were recorded at the wavelength range 800–200 nm. The wavelengths at maximum absorption band (λ_{max}) and the molar absorptivity (ϵ) of the different bands in the recorded spectra of the complexes (cf. Fig. 1) are given in Table 3. The ligand exhibits absorption bands in UV-Vis region around 380 and 430 nm that is assigned to $n \rightarrow \pi^*$ transition originating from the amide or imine function of the Schiff base ligand. Another band observed below 300 nm is assigned to $\pi \rightarrow \pi^*$ transition. The designed complexes display a characteristic band centered at $\lambda_{\text{max}} = 376\text{--}390 \text{ nm}$ ($\epsilon_{\text{max}} = 2667\text{--}3740 \text{ mol}^{-1} \text{ cm}^2$). This band may be mainly ascribed to an intramolecular charge transfer transition taking place in the complexed ligand. Moreover, there is a band shown in the region 414–462 nm ($\epsilon_{\text{max}} = 1113\text{--}3488 \text{ mol}^{-1} \text{ cm}^2$) which that may be attributed to charge transfer from ligand to metal. Furthermore, the $L \rightarrow \text{MCT}$ band is followed by a broad band from 494–520 nm ($\epsilon_{\text{max}} = 704\text{--}1380 \text{ mol}^{-1} \text{ cm}^2$). This band may be mainly attributed to $d \rightarrow d$ transition in an octahedral structure of the prepared complexes [21,52].

3.1.4. Determination of the stoichiometry of the investigated complexes

The stoichiometry of the various complexes formed in solutions via the reaction of Fe(II) with the studied ligands was determined by applying the spectrophotometric molar ratio [53–56] and continuous variation methods [55,56] as shown in Figs. 2 and 3. The curves of continuous variation method (Fig. 2) displayed maximum absorbance at mole fraction $X_{\text{ligand}} = 0.56$ in case of nhi complex, that indicates the formation of complex with metal ion to ligand ratio 1:1. Although in the case of nali, nphali, nasi and nari complexes, the maximum absorbances were obtained at $X_{\text{ligand}} = 0.65\text{--}0.7$ indicating the formation of complexes with metal ion to ligand ratio 1:2 as presented in Schemes 3 and 4. Moreover, the data resulted from applying the mole ratio method support the same metal ion to ligand ratio of the prepared complexes (cf. Fig. 3).

3.1.5. Magnetic moment measurements

Magnetic susceptibility measurements showed that the prepared complexes have paramagnetic character and suggested high spin values (4.18–5.12 BM) i.e., the studied Schiff base amino acid

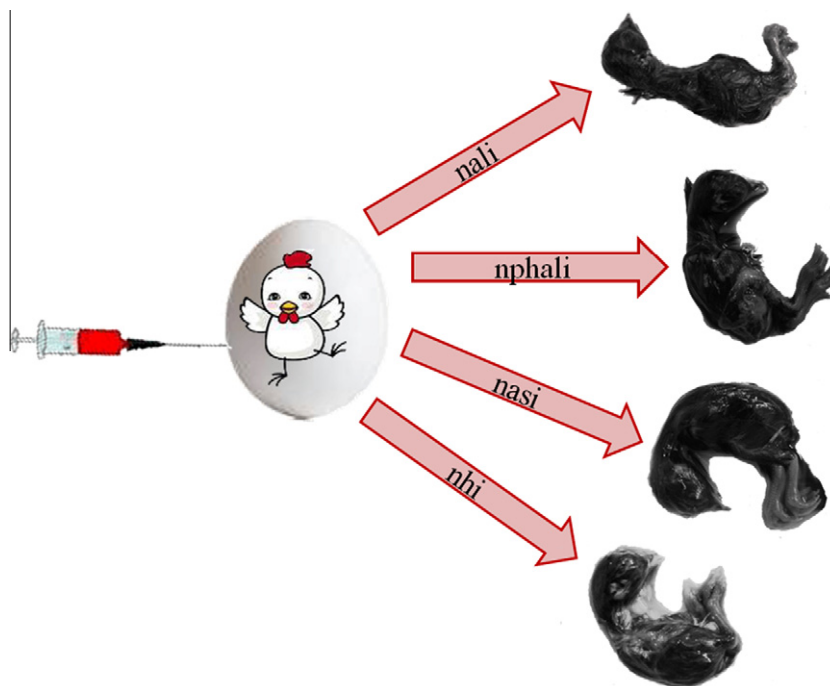


Fig. 5. Photographs of chick embryos exposed to 40 µg/egg of the investigated complexes.

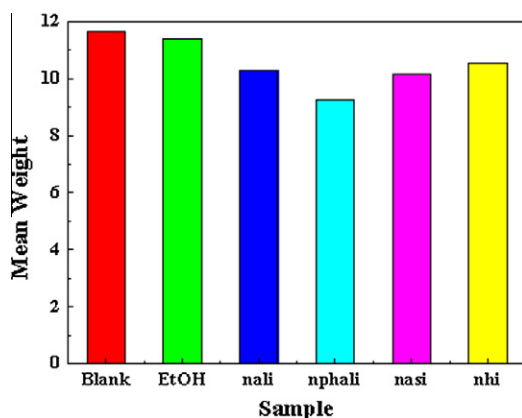


Fig. 6. Mean weight of chick embryos exposed to 100 µg/egg of the investigated complexes.

ligands are so weak that they exhibited low t_{2g} and e_g d-splitting of the octahedral structures of the complexes [57,58].

3.1.6. The formation constants of the investigated complexes

The formation constants (K_f) of the studied Fe(II) Schiff base amino acid complexes formed in solution were obtained from the spectrophotometry measurements by applying the continuous variation method [21,59,60] according to the following relations:

$$K_f = \frac{A/A_m}{(1 - A/A_m)^2 C} \quad \text{in case of 1 : 1 complexes}$$

$$\text{and } K_f = \frac{A/A_m}{4C^2(1 - A/A_m)^3} \quad \text{in case of 1 : 2 complexes}$$

where A_m is the absorbance at the maximum formation of the complex, A is the arbitrary chosen absorbance values on either sides of the absorbance mountain col (pass) and C is the initial concentration of the metal. As mentioned in Table 4, the obtained K_f values indicate the high stability of the prepared complexes. The values

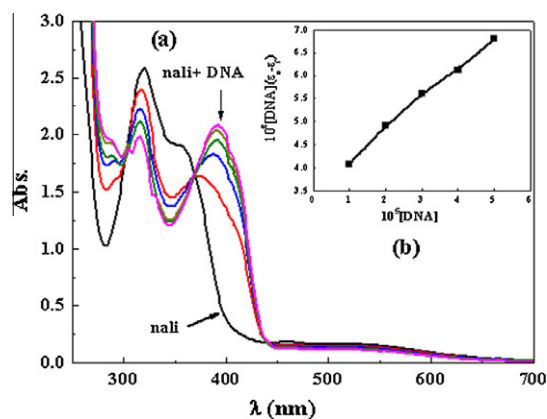


Fig. 7. (a) Spectrophotometer titration of nali complex (10^{-3} M) in 0.01 M Tris buffer (pH 7.5, 25 °C) with CT-DNA (from top to bottom, 0–50 µM DNA, at 10 µM intervals). (b) Plot of $[DNA]/(\epsilon_a - \epsilon_f)$ versus $[DNA]$ for the titration of DNA with nali complex.

of K_f for the studied complexes increase in the following order: $nhi < nasi < nphali < nali < nari$. Moreover, the values of the stability constant (pK) and Gibbs free energy (ΔG°) of the investigated complexes are cited in Table 4.

3.1.7. Stability range of the investigated complexes

The pH-profile (absorbance vs. pH) presented in Fig. 4 showed typical dissociation curves and a wide stability pH range (4–10) of the studied complexes. This means that the formation of the complex greatly stabilizes the Schiff base amino acid ligands. Consequently, the suitable pH range for the different applications of the prepared complexes is from pH = 4 to pH = 10.

3.2. Teratogenicity test of the prepared complexes

In control embryos of 18-days old, the growth morphological features appears normal, head; body covered with feathers and

Table 6
Spectral parameters for DNA interaction with the prepared complexes.

Complex	λ_{\max} free (nm)	λ_{\max} bound (nm)	$\Delta\lambda$ (nm)	Chromism (%) ^a	Type of chromism	Binding constant $K_b \times 10^4 \text{ M}^{-1}$	$\Delta G^\circ \text{ kJ mol}^{-1}$
nali	516	512	4	10.30	Hypo	3.72	-26.07
	346	372	26	16.06	Hypo		
nphali	522	516	6	9.11	Hypo	2.92	-25.49
	350	384	34	16.19	Hypo		
nasi	520	518	2	19.85	Hypo	3.51	-25.93
	382	392	10	10.15	Hyper		
nhi	518	514	4	9.25	Hypo	35.73	-31.68
	363	384	21	14.53	Hypo		
nari	502	498	4	4.06	Hypo	6.02	-27.27
	354	390	36	27.16	Hypo		

^a Chromism(%) = $(A_{\text{free}} - A_{\text{bound}}) / A_{\text{free}}$ [63].

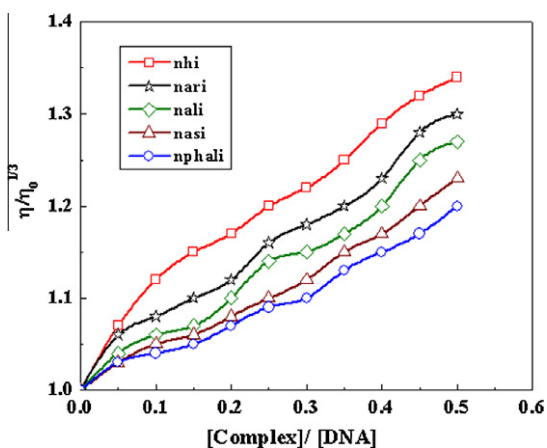


Fig. 8. The effect of increasing the amount of the synthesized complexes on the relative viscosities of DNA at $[\text{DNA}] = 0.5 \text{ mM}$, $[\text{complex}] = 25\text{--}250 \text{ }\mu\text{M}$ and 298 K .

appendages are well developed. The used solvent (5% (v/v) ethanol/water) has no effect on embryos and their formation was 100% at this percent. Thus the difference in the weight of embryos may be attributed to the effect of the investigated complexes. The recent complexes were found to be safe until a concentration of $100 \text{ }\mu\text{g/egg}$ and relatively well developed embryos were noted. In exposed embryos to nphali complex, concentration-dependent embryo resorption was observed. The percentage of resorption was 40% at $200 \text{ }\mu\text{g/egg}$. In addition to embryo resorption that represents a characteristic feature; retarded development of feathers to featherless skin was observed in exposed embryos at $200 \text{ }\mu\text{g/egg}$. From the statistical calculations (cf. Table 5 and Figs. 5 and 6), it was observed that for nali and nhi complexes until a concentration of $20 \text{ }\mu\text{g/egg}$, there is not any significant difference in weight of embryos compared to the control. Moreover, a relatively decrease in the weight of embryos at the concentration range from 40 to $200 \text{ }\mu\text{g/egg}$. Furthermore, there is no significant decrease in the weight of embryos at concentrations of 5 and $10 \text{ }\mu\text{g/egg}$ for nasi complex and at $5 \text{ }\mu\text{g/egg}$ for nphali complex. At the concentration range from 10 to $100 \text{ }\mu\text{g/egg}$ for nphali complex, there is a significant decrease in the weight of embryos compared to the control. This behavior was observed for nasi complex at the concentration range from 20 to $200 \text{ }\mu\text{g/egg}$. It is worth noting that the relative effect of the investigated complexes on the weight of embryos may be mainly ascribed to the influence of the function group.

3.3. DNA-binding studies

Titration with electronic absorption spectroscopy is universally employed and an effective method to investigate the binding mode of DNA with a metal complex [61]. The spectra were recorded as a

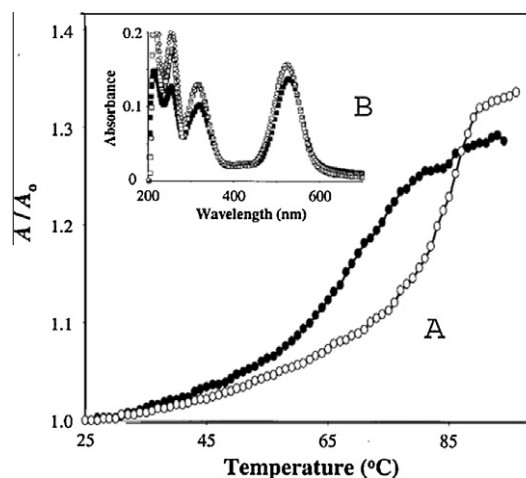


Fig. 9. (a) CT DNA ($3.50 \times 10^{-5} \text{ M}$ in base pairs) melting curves in the absence of nphali (●) and presence of nphali (○) with a 1:1 M ratio of metal complex to DNA base pair in 5 mM Tris, 50 mM NaCl, pH 7.2. (b): UV-vis spectra of nphali ($3.50 \times 10^{-5} \text{ M}$) in the absence and presence of CT DNA (3.50×10^{-5} in base pairs) at $20 \text{ }^\circ\text{C}$ (■) and $85 \text{ }^\circ\text{C}$ (□) in 5 mM Tris, 50 mM NaCl, pH 7.2.

function of the addition of the buffer solutions of pre-treated CT-DNA to the buffer solutions of the complexes. If the binding mode is intercalation, the orbital of intercalated ligand may couple with the orbital of the base pairs, reducing the $\pi\text{--}\pi^*$ transition energy and resulting in bathochromism. If the coupling orbital is partially filled by electrons, it results in decreasing the transition probabilities and resulting in hypochromism [62]. The extent of the hypochromism in the metal-to-ligand charge transfer (MLCT) band is commonly consistent with the strength of intercalative interaction [63]. The electronic absorption spectra of nali complex in the absence and presence of different concentration of buffered CT-DNA are given in Fig. 7. By adding of DNA, the absorption intensities of MLCT band gradually increased. Moreover, addition of increasing amounts of CT-DNA resulted in a decrease of absorbance for each investigated complex. Representative spectra illustrating this hypochromicity and the presence of isosbestic points observed for the interaction of nali with CT-DNA (cf. Fig. 7). Table 6 shows spectra parameters for DNA interaction with the prepared complexes. It can be realized from the high percent of hypochromicity that the high strength binding of the prepared complexes with DNA. The investigated complexes could bind to DNA via an intercalative mode and showed a different DNA cleavage activity with the sequence: $\text{nhi} > \text{nari} > \text{nali} > \text{nasi} > \text{nphali}$. The results revealed that the structure difference on the amino acids may lead to obvious difference of DNA binding and cleavage abilities of the complexes.

Spectroscopic data are necessary, but not enough to support a binding mode. Hydrodynamic methods such as viscosity

measurements, which are sensitive to length increase or decrease of DNA, are regarded as the most powerful means of studying the binding mode of complexes to DNA [64,65].

The relative viscosity of DNA solution increases significantly as the amount of the complex increases, as it is shown in Fig. 8. This can be owing to the insertion of aromatic ring in Schiff base ligand into the DNA base pairs and resulting in a bend in the DNA helix, hence, increase in separation of the base pairs at the intercalation site, consequently increasing in DNA molecular length. Moreover, the sequence of the observed increase in values of viscosity was correlated the binding affinity to DNA i.e. nhi show the highest binding affinity to DNA and the highest viscosity. The information obtained from this work may be helpful to the understanding of the mechanism of the interaction of small molecules with nucleic acids, and should be useful in the development of potential probes of DNA structure and conformation.

3.3.1. Thermodynamic profile of the binding of nphali to DNA

To gain a better understanding of thermodynamics of the reaction between the complex and DNA, it is useful to determine the contributions of enthalpy and entropy of the reaction. The standard enthalpy and entropy, of the binding of nphali to DNA were determined by substituting the experimental data obtained from absorbance titrations and DNA melting studies into van't Hoff's equation and the equations of the standard free energy change. The DNA melting curves of CT-DNA in the absence and in the presence of nphali are presented in Fig. 9. Molecules such as intercalators slot in between base pairs and interact through pi stacking. This has a stabilizing effect on DNA's structure which leads to a raise in its melting temperature. The T_m of CT-DNA was found to be 71 °C, and it was raised to 83 °C in the presence of nphali. Increase in thermal stability of DNA duplex caused by the formation of DNA-intercalator adduct is commonly observed [66]. The absorption spectra of nphali in the presence of CT-DNA at 20 and 90 °C are shown in the of Fig. 9b. Hyperchromism and red shift at 316 and 523 nm were observed as the temperature of solution increased from 20 to 90 °C. Moreover, the absorption spectrum of nphali in the presence of CT-DNA at 90 °C resembled that of in the absence of DNA at 90 °C. These results also establish that the spectral changes accompany the binding of nphali to DNA are reversible and that the chromophore was not destroyed or chemically altered in the binding process [67]. The results support intercalation of nphali into the double-helical DNA. The DNA binding constants of nphali at 83 °C was determined by McGhee's equation [68]:

$$(1/T_m^0 - 1/T_m) = (\Delta H_m/R) \ln(1 + KL)^{1/n}$$

where T_m^0 is the melting temperature of CT-DNA alone, T_m is the melting temperature in the presence of metal complex, ΔH_m is the enthalpy of DNA melting (per bp), R is the gas constant, K is the DNA binding constant at T_m , L is the free ligand concentration (approximated at the T_m by the total ligand concentration), and n is the binding site size. A value of ΔH_m 14.0 ± 0.3 kJ mol⁻¹ was used [69]. On the basis of the neighbor exclusion principle, the n value for nphali was assumed to be 2.0 bp. By substituting the required parameters to McGhee's equation, K was determined to be 4.15 × 10² M⁻¹ at 83 °C for nphali. The standard enthalpy and standard entropy of nphali binding to CT-DNA were determined by van't Hoff's equation and the standard free energy change:

$$\ln(K_1/K_2) = (\Delta H^\circ/R)(T_1 - T_2/T_1T_2)$$

$$\Delta G^\circ = \Delta H^\circ - T\Delta S^\circ$$

where K_1 and K_2 are the DNA binding constants of nphali at temperature T_1 and T_2 , respectively. ΔG° , ΔH° and ΔS° are the standard free energy change, standard enthalpy, and standard entropy of nphali

binding to CT-DNA, respectively. By substituting $K_1 = 3.95 \times 10^4 \text{ M}^{-1}$ ($T_1 = 293 \text{ K}$) and $K_2 = 4.15 \times 10^2 \text{ M}^{-1}$ ($T_2 = 356 \text{ K}$) into van't Hoff's equation, ΔH° is found to be -44.17 kJ mol⁻¹. The standard free energy change is equal -26.22 kJ mol⁻¹ and $\Delta S^\circ = -61.39 \text{ J mol}^{-1} \text{ K}^{-1}$ at 20 °C. Negative binding free energy means that the energy of free complex nphali and DNA is higher than that of the adduct, and the binding of nphali and DNA is favorable at 20 °C. The binding of nphali and DNA is exothermic according to the negative enthalpy. Negative entropy implies that the degree of freedom is decreased after nphali and DNA binding, and it is thermodynamically unfavorable.

4. Conclusion

A new series of Fe(II) tridentate Schiff base amino acid complexes have been synthesized. The Schiff bases derived from o-hydroxynaphthaldehyde and L-alanine (nal), L-phenylalanine (nphal), L-aspartic acid (nas) and L-arginine (nar) are monoanionic tridentate ligands. Results of the physical measurements show that Fe(II) ion is coordinated by two phenolic oxygen atoms, two azomethine N atoms and two carboxylate O atoms to form octahedral complexes with the general formula [Fe(HL)₂].nH₂O. Since, Schiff base ligand of histidine (nh) has an imidazole ring which contains two nitrogen atoms one of that protonates at pH range (6–7), it behaves as dianionic tetradentate and coordinates to Fe(II) to give complex of the general formula [FeL(H₂O)₂].2H₂O. The prepared complexes have non-electrolytic nature. The suggested formulas were confirmed by applying the molar ratio and continuous variation methods. Moreover, the obtained K_f values indicate the high stability of the prepared complexes and their values increase in the following order: nhi < nasi < nphali < nail < nari. Furthermore, the results of embryos toxicity indicate that the investigated complexes are safe until the concentration of 100 µg/chick egg and follow the order nhi > nail > nasi > nphali that enlarge the area of the biological application of the studied Fe(II) Schiff base amino acid complexes. According to the spectrophotometry and viscosity measurements, the prepared complexes bind to DNA via an intercalative mode.

Acknowledgement

The authors are grateful to Dr. Fakhr Lashin, Zoology Department, Faculty of Science, Sohag University for his help in the teratogenicity test.

References

- [1] J. van der Geer, J.A.J. Hanraads, R.A. Lupton, J. Sci. Commun. 163 (2010) 51.
- [2] D.E. Goldberg, V. Sharma, A. Oksman, I.Y. Gluzman, J. Biol. Chem. 272 (1997) 6567.
- [3] A.E. Tai, E.J. Lien, M.M.C. Lai, T.A. Khwaja, J. Med. Chem. 27 (1984) 238.
- [4] P.H. Wang, G.J. Keck, E.J. Lien, M.M.C. Lai, J. Med. Chem. 33 (1990) 608.
- [5] A. Pasini, L. Casella, J. Inorg. Nucl. Chem. 36 (1974) 2133.
- [6] H. Luo, P.E. Fanwick, M.A. Green, Inorg. Chem. 37 (1998) 1127.
- [7] A. Prakash, B.K. Singh, N. Bhojak, D. Adhikari, Spectrochim. Acta A 76 (2010) 356.
- [8] M. El-Beherly, H. El-Twigry, Spectrochim. Acta A 66 (2007) 28.
- [9] Z. Afrasiabi, E. Sinn, W. Lin, Y. Ma, C. Campana, S. Padhye, J. Inorg. Biochem. 99 (2005) 1526.
- [10] M. Sonmez, M. Celebi, I. Berber, Euro. J. Med. Chem. 45 (2010) 1935.
- [11] H.S. Abbo, S.J.J. Titinich, R. Prasad, S. Chand, J. Mol. Catal. A: Chem. 225 (2005) 225.
- [12] K.C. Gupta, A.K. Sutar, J. Mol. Catal. A: Chem. 272 (2007) 64.
- [13] K.C. Gupta, A.K. Sutar, React. Funct. Polym. 68 (2008) 12.
- [14] H. Shyu, H. Wei, G. Lee, Y. Wang, J. Chem. Soc. Dalton Trans. (2000) 915.
- [15] X. Wang, G. Wu, W. Wei, Y. Sun, Catal. Lett. 136 (2010) 96.
- [16] Z. Wu, D. Xu, Z. Feng, Polyhedron 20 (2001) 281.
- [17] D.J. Darensbourg, O. Karroonnirun, Inorg. Chem. 49 (5) (2010) 2360.
- [18] M. Nath, S. Kamaluddin, J. Cheema, Ind. J. Chem. 32A (2) (1993) 108.
- [19] K.C. Gupta, H.K. Abdulkadir, S. Chand, J. Mol. Catal. A: Chem. 202 (2003) 253.

- [20] A.M. Awad, A.M. Shaker, A.B. El-Din Zaki, L.A.E. Nassr, *Spectrochim. Acta A* 71 (2008) 921.
- [21] A.M. Shaker, A.M. Awad, L.A.E. Nassr, *Synth. React. Inorg. Metal-Org. Chem.* 33 (1) (2003) 103.
- [22] N. Thankarajan, K. Mohanan, *J. Ind. Chem. Soc.* LXIII 63 (1986) 861.
- [23] P.K. Sharma, S.N. Dubey, *Indian J. Chem.* 33A (12) (1994) 1113.
- [24] K.E. Erkkila, D.T. Odom, J.K. Barton, *Chem. Rev.* 99 (1999) 2777.
- [25] R. Vijayalakshmi, M. Kanthimathi, V. Subramanian, B.N. Nair, *Biochim. Biophys. Acta* 1475 (2000) 157.
- [26] C. Liu, M. Wang, T. Zhang, H. Sun, *Coord. Chem. Rev.* 248 (2004) 147.
- [27] X.Y. Wang, J. Zhang, K. Li, N. Jiang, S.Y. Chen, H.H. Lin, Y. Huang, L.J. Ma, X.Q. Yu, *Bioorg. Med. Chem.* 14 (2006) 6745.
- [28] N. Raman, J.D. Raja, A. Sakthivel, *J. Chem. Sci.* 119 (4) (2007) 303.
- [29] A.T. Chaviara, E.E. Kioseoglou, A.A. Pantazaki, A.C. Tsipis, P.A. Karipidis, D.A. Kyriakidis, C.A. Bolos, *J. Inorg. Biochem.* 102 (2008) 1749.
- [30] N. Mahalakshmi, R. Rajavel, *Inter. J. Pharm. Technol.* 2 (4) (2010) 1133.
- [31] D. Sabolová, M. Kožurková, T. Plichta, Z. Ondrušová, D. Hudecová, M. Simkovič, H. Paulíková, A. Valent, *Inter. J. Bio. Macromol.* 48 (2011) 319.
- [32] M.S.A. Begum, S. Saha, M. Nethaji, A.R. Chakravarty, *J. Inorg. Biochem.* 104 (2010) 477.
- [33] I. Sakiyan, E. Loğoğlu, S. Arslan, N. Sari, N. Şakiyan, *BioMetals* 17 (2004) 115.
- [34] H.T.S., Britton, *Hydrogen Ions*, fourth ed., vol. 1, Chapman and Hall, 1952.
- [35] J. Murmur, *J. Mol. Biol.* 3 (1961) 208.
- [36] N. Raman, K. Pothiraj, T. Baskaran, *J. Mol. Struct.* 1000 (2011) 135.
- [37] A. Wolf, G.H. Shimer, T. Meehan, *Biochemistry* 26 (1987) 6392.
- [38] S. Satyanarayana, J.C. Dabroniak, J.B. Chaires, *Biochemistry* 31 (1992) 9319.
- [39] K. Nakamoto, *Infrared and Raman Spectra of Inorganic and Coordination Compounds*, fourth ed., vol.3, J. Wiley and Sons, New York, 1986.
- [40] G. Ibrahim, E. Chebli, M.A. Kahan, G.M. Bouet, *Transit. Met. Chem.* 24 (3) (1999) 294.
- [41] K.-Y. Choi, Y.-M. Jeon, H. Ryu, J.-J. Oh, H.-H. Lim, M.-W. Kim, *Polyhedron* 23 (6) (2004) 903.
- [42] P.K. Sharma, S.N. Dubey, *Proc. Ind. Acad. Sci. (Chem. Sci.)* 106 (1) (1994) 23.
- [43] J.P. Lambert, H.F. Shurvell, L. Verbit, R.C. Cooks, G.H. Stout, *Organic Structural Analysis*, vol. 326, Macmillan Publishing Co. Inc., and Collier Macmillan Publishers, New York and London, 1968.
- [44] M.S.A. Begum, S. Saha, M. Nethaji, A.R. Chakravarty, *J. Inorg. Bio. Chem.* 104 (2010) 477.
- [45] K. Nakamoto, *Infrared and Raman Spectra of Coordination Compounds*, John Wiley, New York, 1978.
- [46] P. Teyssie, J.J. Charette, *Spectrochim. Acta* 9 (19) (1963) 1407.
- [47] J.S. Gruber, M.C. Harris, E. Sinn, *J. Inorg. Nucl. Chem.* 30 (1968) 1805.
- [48] A.M. Abdel-Mawgoud, *Synth. Inorg. Met. Org. Chem.* 28 (4) (1998) 555.
- [49] B. Singh, R.D. Singh, *J. Chem. Soc.* 60 (1982) 861.
- [50] N. Saha, D. Bhattacharya, *Indian J. Chem. A* 21 (1982) 648.
- [51] L.H. Abdel-Rahman, L.P. Battaglia, P. Sgarabotto, M.R. Mahmoud, *J. Chem. Crystallogr.* 24 (9) (1994) 567.
- [52] A.B.P. Lever *Inorganic Electronic Spectroscopy*, vol. 298, Elsevier Publishing, Amsterdam, 1968.
- [53] J.H. Yoe, A.L. Jones, *Ind. Eng. Chem. (Analyst. Ed.)* 16 (1944) 111.
- [54] R. El-Shiekh, M. Akl, A. Gouda, W. Ali, *J. Am. Sci.* 7 (4) (2011) 797.
- [55] S.S. Shah, R.G. Parmar, *Der Pharma Chemica* 3 (1) (2011) 318.
- [56] P. Job, *Ann. Chem.* 9 (1928) 113.
- [57] E. Canpolat, M. Kaya, *J. Coord. Chem.* 55 (2002) 961.
- [58] A.S. El-Tabl, *J. Coord. Chem.* 61 (15) (2008) 2380.
- [59] I.M. Issa, R.M. Issa, M.S. Abd-elalil, *Egypt. J. Chem.* 14 (1) (1971) 25.
- [60] R.M. Issa, A.A. Hassanein, I.M. El-Mehasseb, R.I. Abed, *Spectrochim. Acta Part A* 65 (2006) 206.
- [61] J.M. Kelly, A.B. Tossi, D.J. McConnell, C.O. Uigin, *Nucl. Acids Res.* 13 (1985) 6017.
- [62] A.M. Pyle, J.P. Rehmann, R. Meshoyrer, C.V. Kumar, N.J. Turro, J.K. Barton, *J. Am. Chem. Soc.* 111 (1989) 3051.
- [63] X.W. Liu, J. Li, H. Li, K.C. Zheng, H. Chao, L.N. Ji, *J. Inorg. Biochem.* 99 (2005) 2372.
- [64] B.C. Baguley, M. LeBret, *Biochemistry* 23 (1984) 937.
- [65] Y. Liu, W. Mei, J. Lu, H. Zhao, L. He, F. Wu, *J. Coord. Chem.* 61 (2008) 3213.
- [66] D.P. Remeta, C.P. Mudd, R.L. Berger, K.J. Breslauer, *Biochemistry* 32 (1993) 5064.
- [67] C.V. Kumar, E.H. Asuncion, *J. Am. Chem. Soc.* 115 (1993) 8547.
- [68] J.D. McGhee, *Biopolymers* 15 (1976) 1345.
- [69] J.B. Chaires, F. Leng, T. Przewloka, I. Fokt, Y.-H. Ling, R. Perez-Soler, W. Priebe, *J. Med. Chem.* 40 (1997) 261.